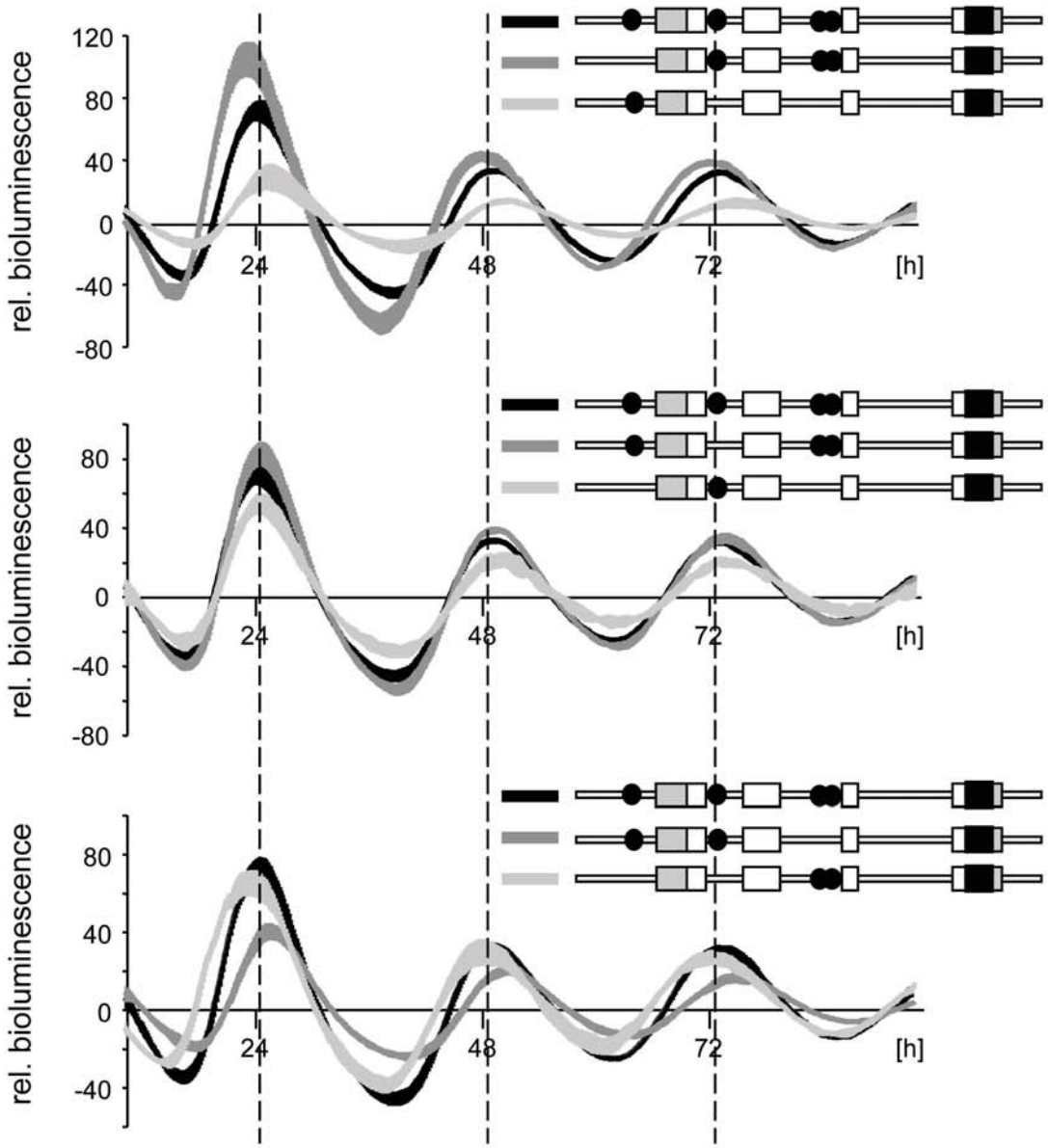

Supplemental Fig. 1. Analysis of the circadian phase of the different *Dbp* reporter constructs. The luciferase recordings were detrended using the LumiCycle software. The indicated constructs were compared to the wild-type construct (black). The numbers on the x-axis represent the time passed after the synchronization of the cultures with dexamethasone. The symmetry of the second and third peaks indicates that the period lengths do not differ between the different recordings. Shown is the average of four experiments ± S.D..

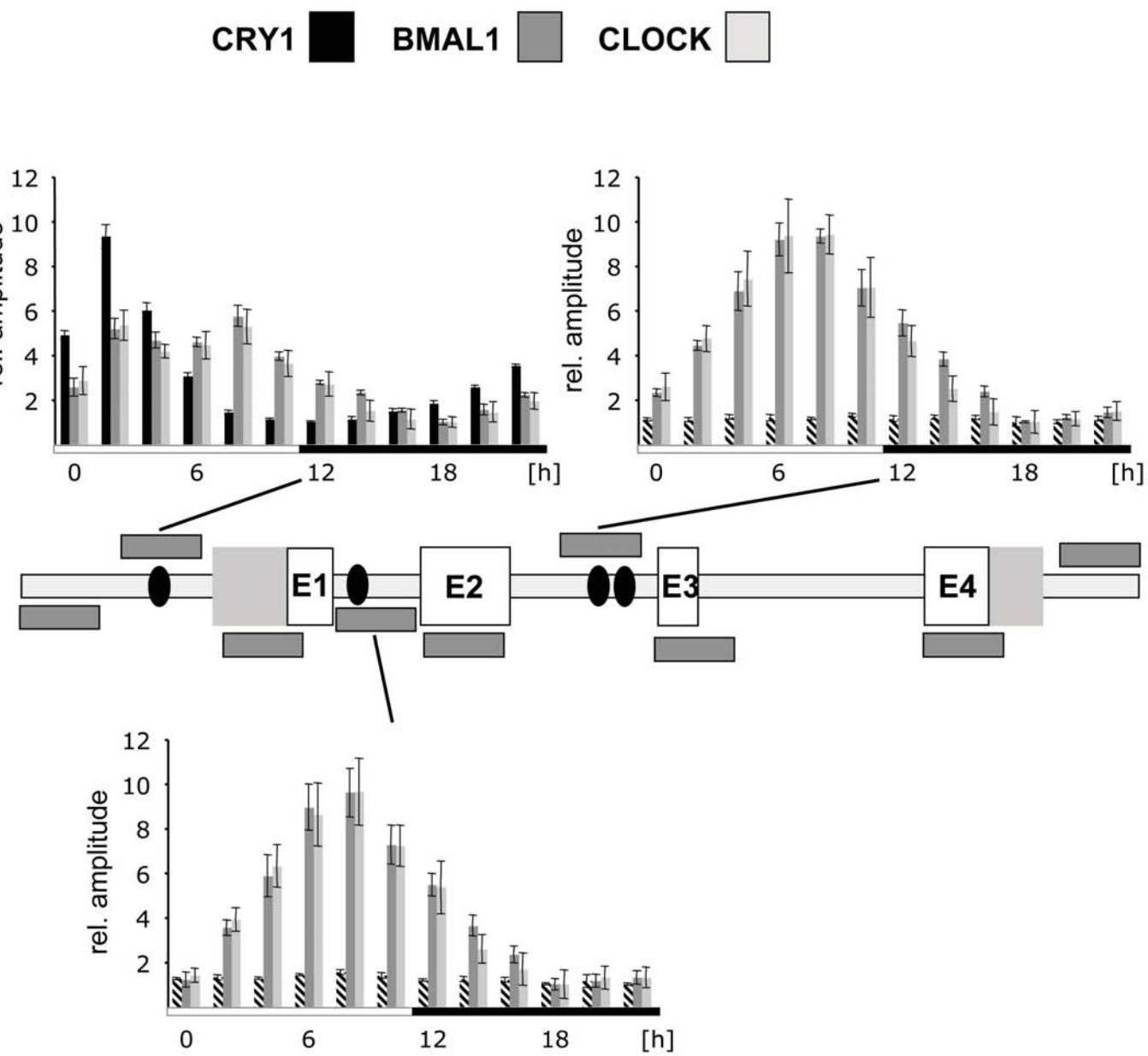

Supplemental Fig. 2. Mapping of binding regions for CRY1, BMAL1 and CLOCK in the *Dbp* gene. Nine distinct regions within the *Dbp* gene were analyzed for the in vivo binding of the indicated proteins by chromatin immunoprecipitation assays. The TaqMan-real time PCR probes covering the entire mouse *Dbp* gene have been described previously (Ripperger and Schibler 2006). Shown are the relative amplitudes of binding of CRY1, BMAL1, and CLOCK to the promoter, the intron 1, or intron 2 regions. The minimum of binding was defined as 1. A bar below each graph represents the light:dark phase. Stripped bars represent regions of background binding for CRY1. Shown is a scheme of the mouse *Dbp* gene (E1 to E4: exons 1 to 4) with the location of the E-box motifs as black ovals (adapted

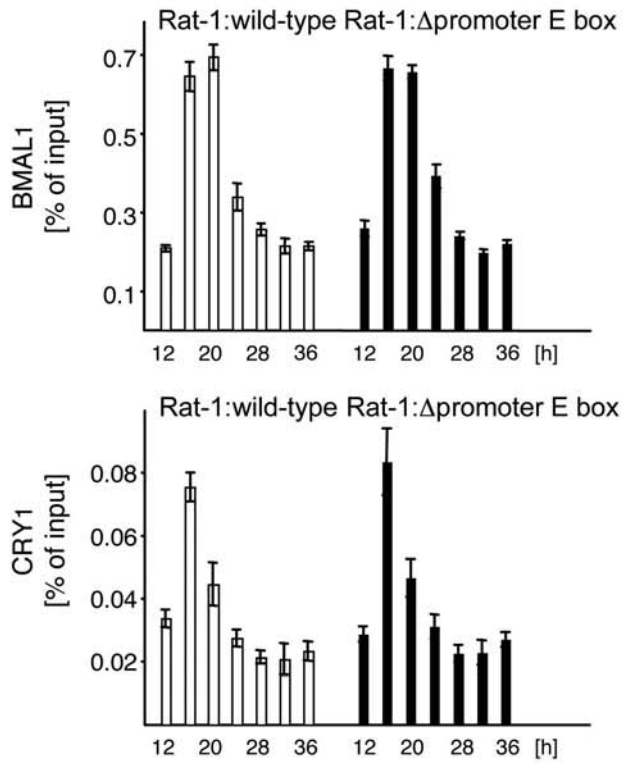

Supplemental Fig. 3. Binding of BMAL1 and CRY1 to the endogenous *Dbp* gene in Rat-1 fibroblasts. Chromatin immunoprecipitation assay to analyze the in vivo binding of either factor to the endogenous rat *Dbp* gene. The TaqMan-real time PCR probes discriminating between the mouse *Dbp* transgene and the rat endogenous gene have been described previously (Ripperger and Schibler 2006). This is a control experiment for Fig. 3B to demonstrate that the ability of BMAL1 and CRY1 to bind to E-box motifs in general is not affected in the Rat-1:Δpromoter E box-stable cell line.

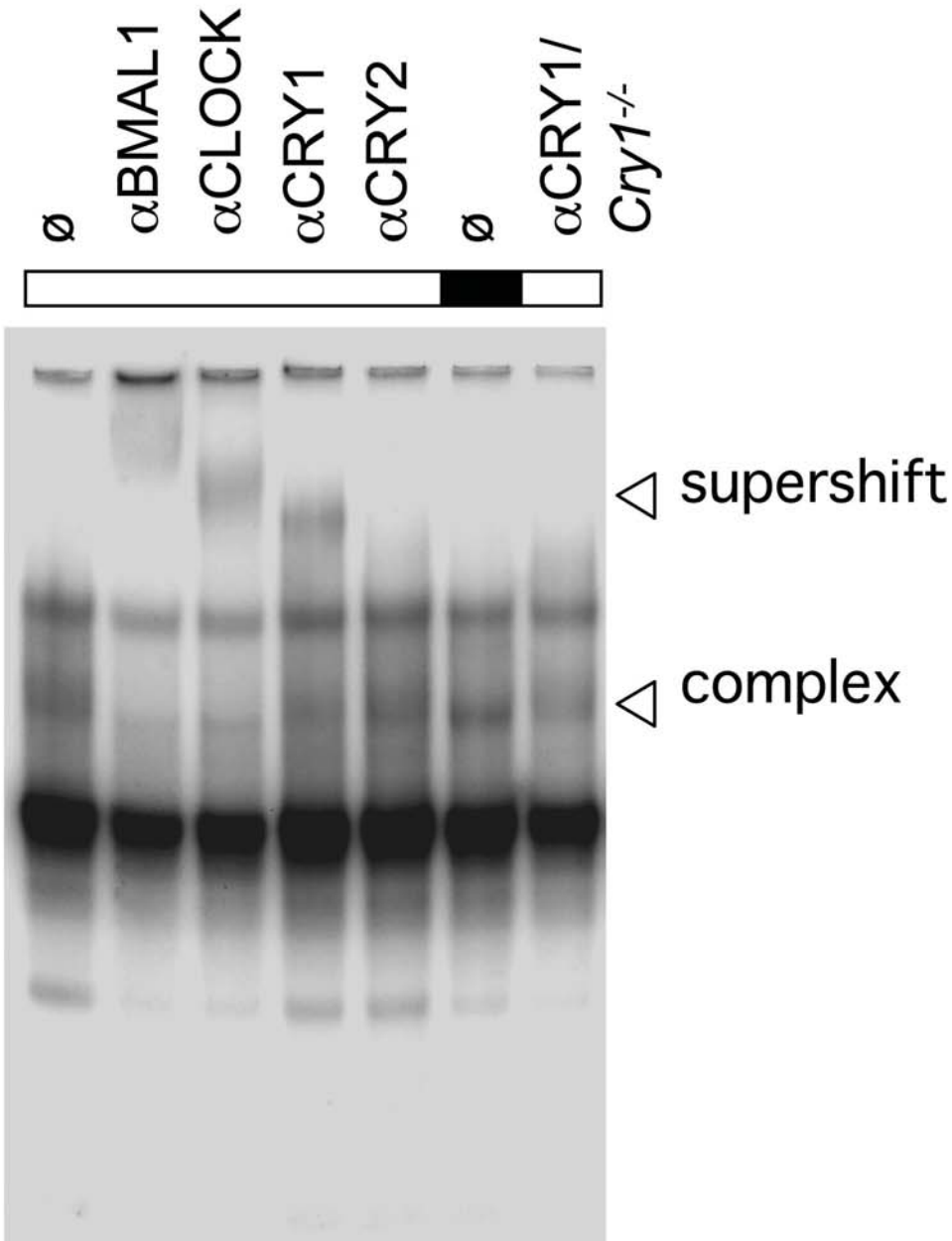

Supplemental Fig. 4. CRY1 binds to the promoter E-box motif in vitro. Nuclear extracts were prepared from wild-type or *Cry1*-deficient mice at ZT3 (white bars) or ZT15 (black bar). Gel mobility shift experiments were performed as described (Ripperger and Schibler 2006), using the indicated antibodies to supershift components of the protein: DNA complexes. Triangles indicate the position of the BMAL1 and CLOCK complexes and the supershift complexes. Note, that without a positive control available yet, the non-binding of CRY2 to this oligonucleotide has to be taken with caution.

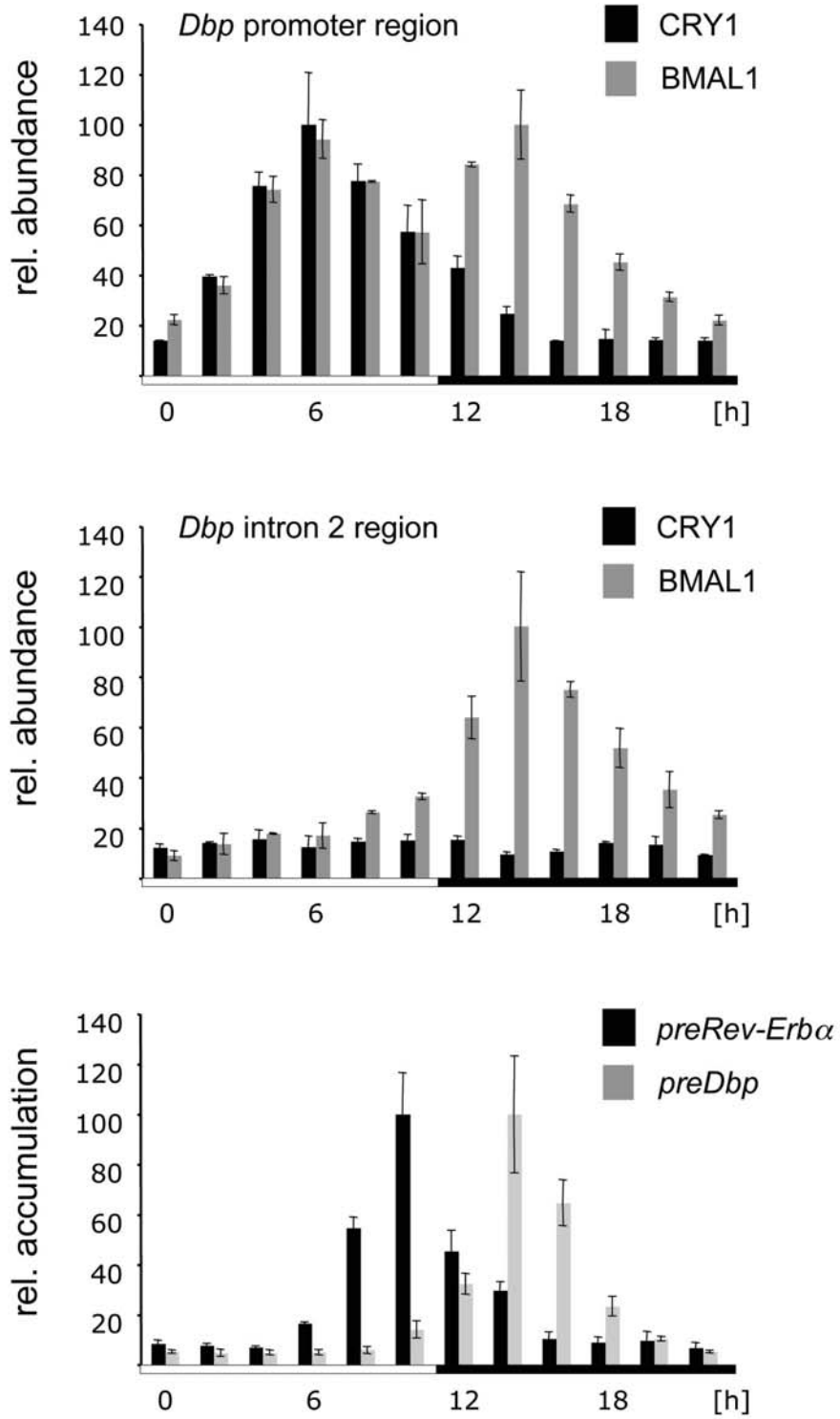

Supplemental Fig. 5. The expression of *Dbp* is delayed compared to *Rev-Erbα* in *Cry2*-deficient mice. Upper two panels: chromatin immunoprecipitation with the indicated antibodies and TaqMan-RT probes for two different regions of the *Dbp* gene. The maximum of CRY1 and BMAL1 binding to the *Dbp* promoter region were set to 100 %. Lower panel: precursor RNA accumulation in liver

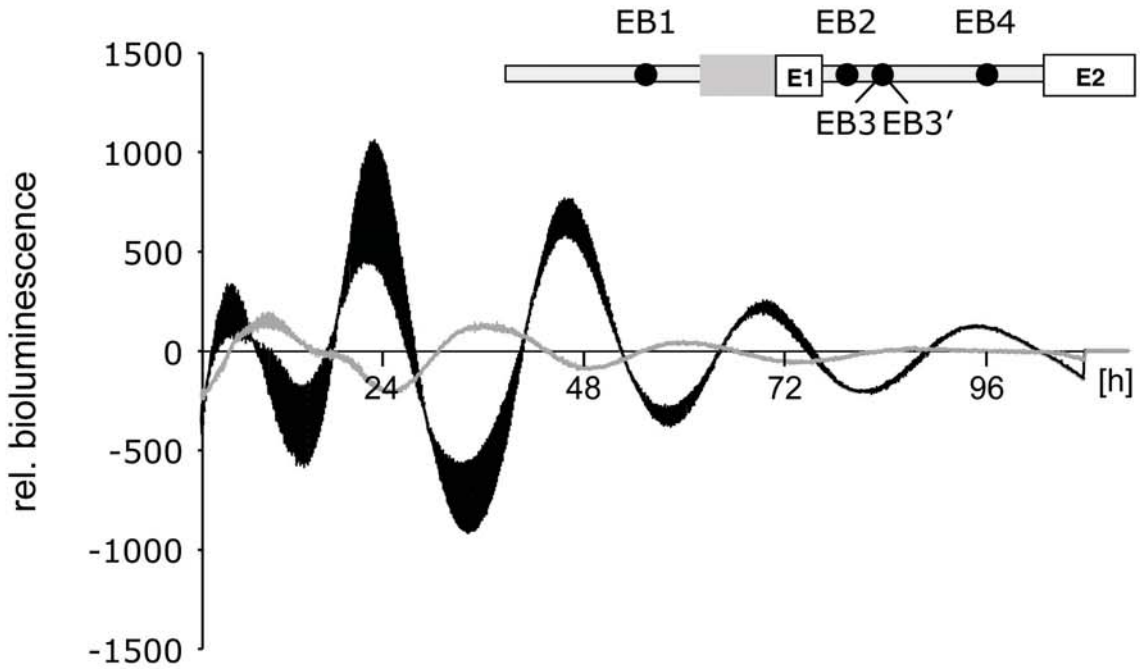

Supplemental Fig. 6. Circadian regulation of the *Rev-Erbα* reporter without functional E-box motifs is in antiphase to the wild-type construct. Detrended data from Fig. 5A. Shown is the time after synchronization of the cells with dexamethasone. Above is shown a scheme of the regulatory region of the *Rev-Erbα* gene with exon 1 and exon 2 and the positions of five potential E-box motifs (black circles).

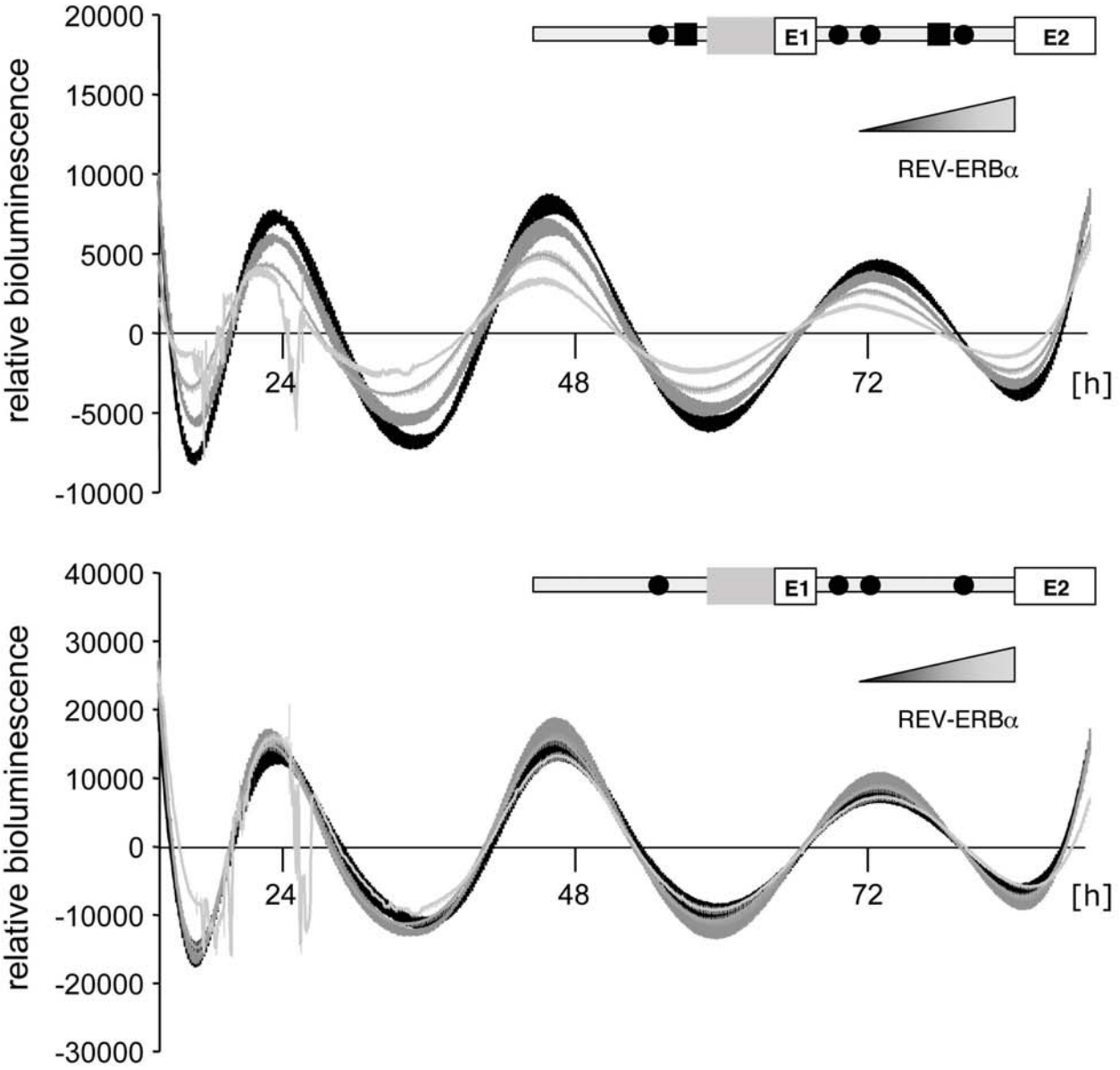

Supplemental Fig. 7. REV-ERBα represses *Rev-Erbα* luciferase expression in a dose-dependent fashion. Detrended data from the experiment shown in Fig. 5B. Upper panel: co-transfection with the wild-type *Rev-Erbα* luciferase reporter; lower panel: co-transfection with the *Rev-Erbα* luciferase reporter without the potential RREs. The gray-scale of the ramp represents increasing amounts of *Rev-Erbα* expression vector (22 ng, 66 ng, or 200 ng). Black circles indicate the position of potential E-box motifs, black squares the position of potential RREs. Note the impact of REV-ERBα on the phase and amplitude of the wild-type but not the mutated construct.

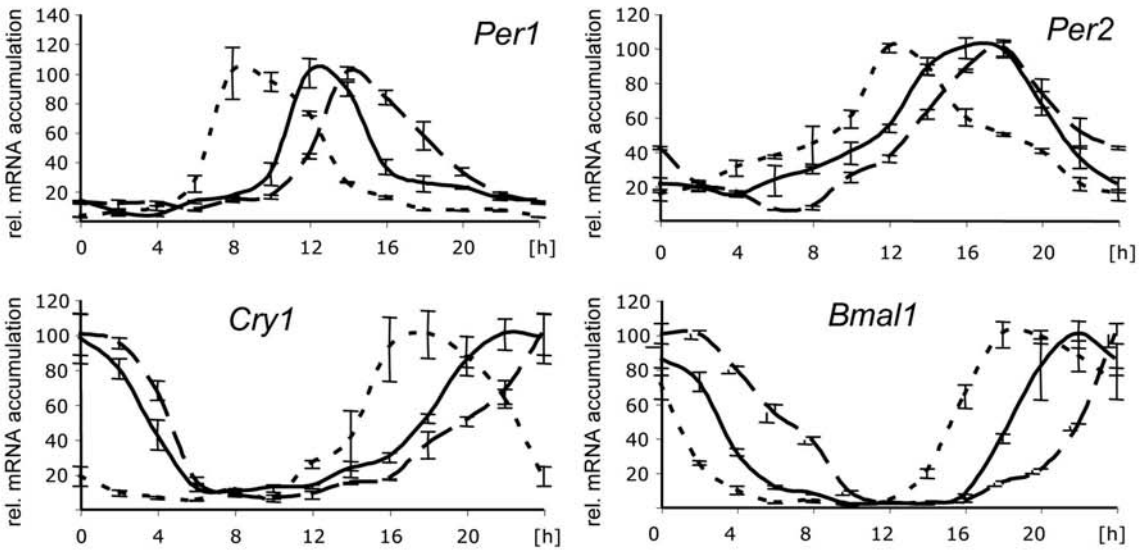

Supplemental Fig. 8. The expression of components of the liver circadian oscillator is modulated to fit into a new photoperiod. Liver mRNA accumulation was measured at two-hours resolution for the indicated genes relative to *Gapdh* accumulation. Dotted lines: SP, 8-hours light/16-hours dark; solid lines: NP, 12-hours light/12-hours dark; hatched lines: LP, 16-hours light/8-hours dark. For better comparison, all peaks were set to 100 % and there is a time scale starting from the transition from the light to the dark phase (ZT0) in hours depicted under the graphs. Average of three experiments ± S.D.. The first value, ZT0, is double-plotted at the end of the line as ZT24.

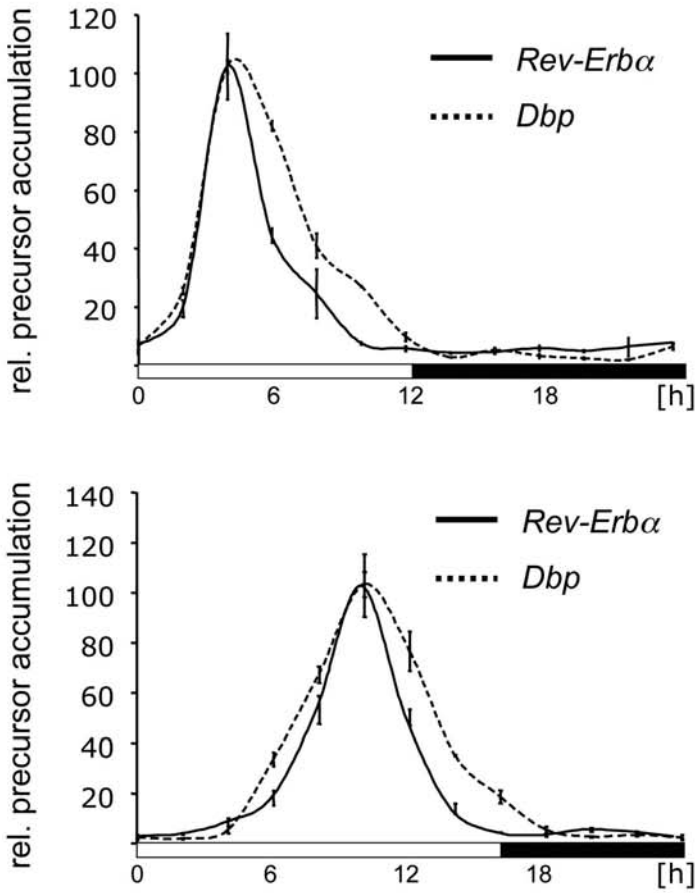

Supplemental Fig. 9. Expression of *Rev-Erbα* and *Dbp* precursor mRNA in *Cry1*-deficient mice. The precursor mRNA for *Rev-Erbα* (solid lines) and *Dbp* (dashed lines) were compared relative to *Gapdh* mRNA accumulation. Data were obtained at two-hours resolution in NP (upper panel) or LP (lower panel). The peaks of precursor mRNA accumulation were set to 100 %. Average of three experiments ± S.D.. The first value, ZT0, is double-plotted at the end of the line as ZT24. Note, that the peaks of precursor mRNA accumulation stay coupled independent of the photoperiod in the livers of these mice.

Supplemental table S1		
Gene	Position	**E'box** **E box**
*Dbp*_promoter	-166	5'-CATCCGATAG**CACGCG**CAA AGC**CATGTG**CTTCCCCCTT-3' 3'-GTAGGCTATC**GTGCGC**GTT TCG**GTACAC**GAAGGGGGAA-5'
*Dbp*_intron2	+2,398	5'-ACCAGTGCTG**CACATT**CCCTCGC**CACGTG**AGTCCGCCTT-3' 3'-TGGTCACGAC**GTGTAA**GGGAGCG**GTGCAC**TGAGGCGGAA-5'
*Rev-Erbα*_promoter	-484	5'-AAACCTAGCA**AACGTG**AGAGCTT**CACGTG**ATTGGAGAAC-3' 3'-TTTGGATCGT**TTGCAC**TCTCGAA**GTGCAC**TAACCTCTTG-5'
*Rev-Erbα*_intron1	+1,353	5'-CAGCTGGCCT**CACGTC**CCCACTC**CACGTG**TGCCCCTCGC-3' 3'-GTCGACCGGA**GTGCAG**GGGTGAG**GTGCAC**ACGGGGAGCG-5'

Alignment of E'-box and E-box sequence motifs (Nakahata et al. 2008; Paquet et al. 2008) found in the mouse *Dbp* and *Rev-Erbα* genes. Indicated are the approximate positions relative to the transcriptional start site. The sequences of the *Rev-Erbα* gene are shown in their anti-sense configuration to allow for a better comparison. Note the difference in the spacing between the E'-box and E-box sequence motifs in the *Dbp* promoter (n = 6; we introduced a space for a better alignment) and the other sites (n = 7), and the high similarity of the *Dbp* intron 2 sequence motif with the *Rev-Erbα* intron 1 sequence motif.

Supplemental table S2	
Gene/ name	Sequence (5' to 3')
*Rev-Erbα*_pro_FW	TCACATGGTACCTGCTCCAG
*Rev-Erbα*_pro_RV	CTTTTGCCCGAGCCTTTC
*Rev-Erbα*_pro_TM	FAM-ACAGAGGGCTCTGCGCAGGC-BHQ1
*Rev-Erbα*_in1_FW	CCCTGACCAACCTTGAGCTA
*Rev-Erbα*_in1_RV	CATGTCTTGCTCACCCACTG
*Rev-Erbα*_in1_TM	FAM-AAGGTTGCCCTGCCTGGTTTAGTG-BHQ1
*Dbp*_pro_FW	ACACCCGCATCCGGTAGC
*Dbp*_pro_RV	CCACTTCGGGCCAATGAG
*Dbp*_pro_TM	FAM-CGCGCAAAGCCATGTGCTTCC-BHQ1
*Dbp*_in1_FW	ATGCTCACACGGTGCAGACA
*Dbp*_in1_RV	CTGCTCAGGCACATTCCTCAT
*Dbp*_in1_TM	FAM-CCTAGTTTCCATGTGACCCTGCGAGG-BHQ1
*Gapdh*_FW	CATGGCCTTCCGTGTTCCTA
*Gapdh*_RV	CCTGCTTCACCACCTTCTTGA
*Gapdh*_TM	FAM-CCGCCTGGAGAAACCTGCCAAGTATG-BHQ1
Cloning of the *Dbp* intron 2 E box into pGL4.24. The phosphorylated double-stranded oligonucleotides containing two copies of the E box (bold) and two copies of the E' box (underlined) were ligated in the presence of an excess of *BamHI* and *BglII* restriction endonucleases. The ligation products were separated on a 2 % agarose gel, 1, 2, or 3 copies eluted and ligated into the *BamHI* site of pGL4.24.	
GATCCGTGCTGCACATTCCCTCGC**CACGTG**AGTGTGCTGCACATTCCCTCGC**CACGTG**AGTA GCACGACGTGTAAGGGAGCG**GTGCAC**TCACACGACGTGTAAGGGAGCG**GTGCAC**TCATCTAG	

Primers user for TaqMan RT-PCR. FAM: 6-fluorescein; BHQ1: black hole quencher 1. Probes located in the intron 1 were also used to measure precursor mRNA accumulation.